Title
Effect of Anion Size on Conductivity and Transference Number of Perfluoroether Electrolytes with Lithium Salts

Journal
Journal of The Electrochemical Society, 164(14)

ISSN
0013-4651

Authors
Shah, Deep B
Olson, Kevin R
Karny, Adar
et al.

Publication Date
2017

DOI
10.1149/2.0301714jes

Peer reviewed

Effect of Anion Size on Conductivity and Transference Number of Perfluoroether Electrolytes with Lithium Salts

Deep B. Shah,[a,b] Kevin R. Olson,[c,*] Adar Karny,[a,b] Sue J. Mecham,[c] Joseph M. DeSimone,[c,d] and Nitash P. Balsara[a,b,e,,z]**

[a]*Department of Chemical and Biomolecular Engineering, University of California, Berkeley, California 94720, USA*
[b]*Materials Science Division, Lawrence Berkeley National Laboratory, Berkeley, California 94720, USA*
[c]*Department of Chemistry, University of North Carolina at Chapel Hill, Chapel Hill, North Carolina 27599, USA*
[d]*Department of Chemical and Biomolecular Engineering, North Carolina State University, Raleigh, North Carolina 27695, USA*
[e]*Environmental Technologies Division, Lawrence Berkeley National Laboratory, Berkeley, California 94720, USA*

Mixtures of perfluoropolyethers (PFPE) and lithium salts with fluorinated anions are a new class of electrolytes for lithium batteries. Unlike conventional electrolytes wherein electron-donating oxygen groups interact primarily with the lithium cations, the properties of PFPE-based electrolytes appear to be dependent on interactions between the fluorinated anions and the fluorinated backbones. We study these interactions by examining a family of lithium salts wherein the size of the fluorinated anion is systematically increased: lithium bis(fluorosulfonyl)imide (LiFSI), bis(trifluoromethanesulfonyl)imide (LiTFSI) salts and lithium bis(pentafluoroethanesulfonyl)imide (LiBETI). Two short chain perfluoroethers (PFE), one with three repeat units, C6-DMC, and another with four repeat units, C8-DMC were studied; both systems have dimethyl carbonate end groups. We find that LiFSI provides the highest conductivity in both C6-DMC and C8-DMC. These systems also present the lowest interfacial resistance against lithium metal electrodes. The steady-state transference number (t^{+}_{ss}) was above 0.6 for all of the electrolytes and was an increasing function of anion size. The product of conductivity and the steady-state transference number, a convenient measure of the efficacy of the electrolytes for lithium battery applications, exhibited a maximum at about 20 wt% salt in all electrolytes. Amongst the systems studied, LiFSI/PFE mixtures were the most efficacious electrolytes.
 [DOI: 10.1149/2.0301714jes]

Manuscript submitted October 2, 2017; revised manuscript received November 2, 2017. Published November 15, 2017.

As applications for rechargeable lithium batteries continue to increase in number, there are added demands for improving the safety and performance. One way of increasing safety is by replacing the flammable electrolytes used in current batteries with nonflammable materials. Current electrolytes comprise mixtures of alkyl carbonates and lithium hexafluorophosphate.[1–3] The alkyl carbonates contain electronegative oxygen atoms that solvate lithium ions. The use of fluorinated anions such as hexafluorophosphate stems from the electronegativity of fluorine, enhanced charge delocalization and ion dissociation. Mixtures of oligomeric and long chain polyethylene oxide and lithium bis(trifluoromethanesulfonyl)imide (LiTFSI) have also been studied for lithium battery applications. These electrolytes also contain electronegative oxygen atoms and lithium salts with fluorinated anions. In order to increase performance and energy capacity of Li-ion systems, cathodes with high operating potentials (5 V vs. Li^+/Li) have been proposed.[4] However, common battery electrolytes, like ethylene carbonate and dimethyl carbonate, decompose above 4.5 V vs. Li^+/Li.[5] Fluorinated compounds have been shown to have larger stability windows, thereby allowing the use of high operating potential cathodes.[6]

This paper is part of a series wherein we examine the possibility of using fluorinated oligomers to dissolve lithium salts with fluorinated anions.[7–11] Our hypothesis is that salt solubility in these systems stems from interactions between the oligomers and the anion. It is known that fluorinated compounds are often only miscible in each other; this is often referred to as the fluorous effect.[12] While the fluorous effect is usually used to describe the mixing of neutral species, there is evidence of similar effects in mixtures of fluorinated ionic compounds and fluorinated polymers.[13] Our work is a departure from the traditional approach of exploiting interactions between the solvent and the cation. The oligomers used in this study are perfluoroethers (PFE) with dimethyl carbonate end groups. The chemical formulae are given in Figure 1 and we refer to them as C6-DMC and C8-DMC. Our electrolytes comprise mixtures of these PFEs and three lithium salts. In addition to LiTFSI, we have also used lithium bis(fluorosulfonyl)imide (LiFSI) and lithium bis(pentafluoroethanesulfonyl)imide (LiBETI). The chemical formulae of the salts used in this study are also given in Figure 1. Our study thus examines the effect of PFE chain length and anion size on ion transport. We characterize ion transport by measuring conductivity using ac impedance and the approximate cation transference number using the steady-state current method.[14–16] We also report on the interfacial impedance between PFE electrolytes and lithium metal electrodes.

A large majority of studies on PEO-based electrolytes use LiTFSI as the salt.[17–19] While these electrolytes exhibit reasonable conductivity at room temperature and lithium salts can be dissolved at high concentrations, the transference number based on the steady-state current method can be as low as 0.05.[20] This is due to specific interactions between the solvent and the cation. A consequence of our hypothesis that the properties of PFE electrolytes are governed by interactions between the solvent and the anion is the expectation that these systems should exhibit significantly higher transference numbers. In this work, we compare ion transport properties of PFE-based electrolytes with literature values of PEO-based electrolytes.

As can be seen in Figure 1, the PFEs used in this study are fluorinated analogs of oligomeric PEOs, triglyme and tetraglyme. The properties of these two classes of electrolytes will differ dramatically for several reasons: (1) The fluorine atoms in PFE, which replace hydrogens in PEO, are actually similar to oxygen atoms in terms of size and electronegativity. (2) Steric effects will differ because C-F bonds are longer and occupy significantly more space than C-H bonds.[21] (3) Interfacial impedance will be impacted by differences in the spontaneous reactions between the electrolytes and lithium metal, and the fact that the C-F bond is stronger than the C-H bond. Our study sheds some light on the effect of these differences on ion transport.

Experimental

PFE synthesis.—The PFEs were synthesized from diol terminated precursors following procedures described in Wong, D. et al. and Olson, K. et al.[7,11] Scheme 1 shows our approach to synthesize C6-DMC. (The approach for synthesizing C8-DMC is essentially identical.) 0.10 mol of the perfluorinated glycol precursor (0.20 mol

*Electrochemical Society Student Member.
**Electrochemical Society Member.
[z]E-mail: nbalsara@berkeley.edu

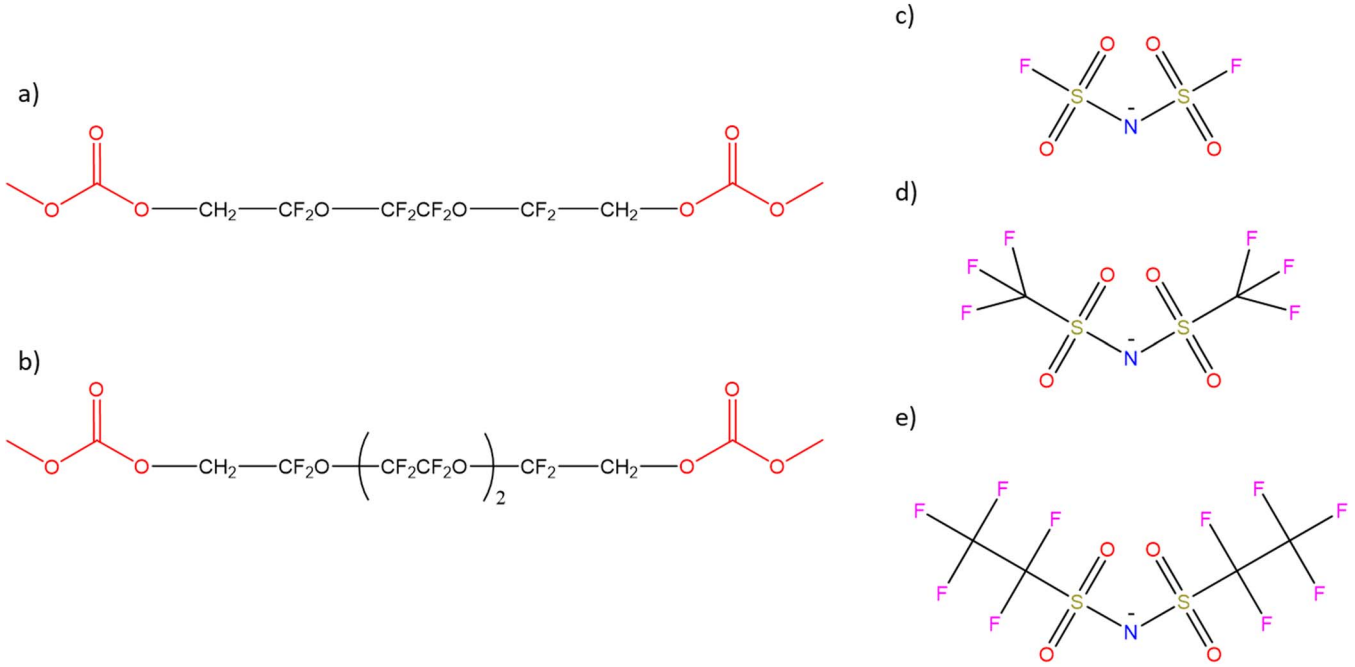

Figure 1. a) C6GDMC, b) C8GDMC, c) FSI anion, d) TFSI anion, and e) BETI anion.

-OH end groups) and three molar equivalents triethylamine (84 mL, 0.60 mol) were dissolved in 400 mL of 1,1,1,3,3-pentafluorobutane in a 1 L 3-neck round-bottom flask. The solution was cooled to 0°C under nitrogen atmosphere. Methyl chloroformate (46 mL, 0.60 mol) was added dropwise over the course of two hours with rapid stirring, resulting in significant gas evolution and formation of the white triethylamine hydrochloride (TEA HCl) precipitate. The reaction was stirred overnight under nitrogen atmosphere at ambient temperature, and reaction completion was confirmed by Fourier-transform infrared spectroscopy.

The TEA HCl salt was removed by gravity filtration, yielding a pale-yellow solution. The salt was washed 3x with 50 mL 1,1,1,3,3-pentafluorobutane to remove residual product. The combined pentafluorobutane solution was then washed 3x with 500 mL water and 1x with 500 mL brine using a separatory funnel. The solution was stirred with activated carbon to remove coloration and dried with magnesium sulfate. After filtering the solids, pentafluorobutane was removed under reduced pressure, yielding a clear, faintly yellow oil. The dimethyl carbonate terminated perfluorinated triethylene- and tetraethylene ethers (C6-DMC and C8-DMC, respectively) were dried under vacuum at 50°C for 2 days. The molecular weight (MW) for C6-DMC is 410 g/mol and that of C8-DMC is 526 g/mol. Figures S1 and S2 in the supplemental information show the NMR spectra of the final products dissolved in deuterated acetone.

Thermogravimetric analysis (TGA) was used to determine the volatility of C6-DMC and C8-DMC using a TA Instruments Q5000 TGA under nitrogen flow (10 mL/min) from 25°C to 500°C at a heating rate of 10°C/min. The temperatures at which a 5% mass loss were recorded from the TGA curves were 126 and 129°C for C6-DMC and C8-DMC. Closed-cup flash point measurements were performed using an Erdco Rapid Tester small-scale apparatus following ASTM D 3278. No flash point was detected for C6-DMC or C8-DMC within the experimental window (up to 250°C).

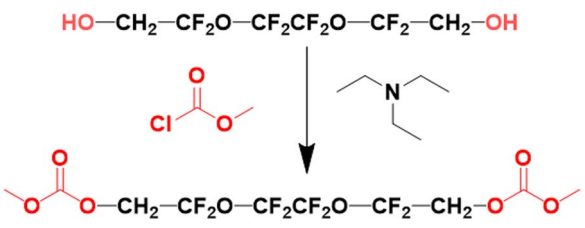

Scheme 1. Reaction to produce C6-DMC form the commercial C6-Diol analog. Conversion of the C8-Diol analog proceeds through the same reaction scheme to produce C8-DMC.

Salts.—Lithium bis(fluorosulfonyl)imide (cat. no. 097602) and lithium bis(pentafluoroethanesulfonyl)imide (cat. no. 080110) were purchased from Oakwood Products, Inc. Both salts were ≥ 99% pure, as confirmed by a Certificate of Analysis form. Lithium bis(trifluoromethanesulfonyl)imide was purchased from Novolyte and was also reported to be ≥ 99% pure. All three salts were dried at 120°C under dynamic vacuum for three days inside a glove box antechamber. All salts, oligomers, and electrolytes were stored within an argon filled Vac glove box with H_2O and O_2 concentrations kept below 1 ppm.

Electrolyte preparation.—Prior to being brought into the glove box, the oligomers were dried under active vacuum inside the glove box antechamber at 50°C for 72 hours. In order to form electrolytes, a predetermined amount of Li salt was added to a known mass of either oligomer. Once the salt was added, the electrolytes were placed on a stir plate and were allowed to mix for 12 hours or more using a magnetic stir bar.

Experimental characterization.—Conductivity samples were prepared by sandwiching an electrolyte soaked separator, Celgard 2500 (Celgard Company), with a stainless steel shim (MTI Corporation) on either side. The stainless steel shims were 15.5 mm in diameter and 0.2 mm in thickness; Celgard 2500 was cut to 19 mm in diameter and had an average thickness of 25.4 ± 0.6 μm. The thickness of the separator was measured for each sample. The stack was placed into CR2032 coin cells (Pred Materials) that were than hermetically sealed. Three replicate cells were produced and measured for each electrolyte. Conductivity data was collected through ac impedance spectroscopy performed on a Bio-Logic VMP3 potentiostat. The frequency range analyzed was between 1 MHz and 100 mHz at an amplitude of 60 mV. Figure 2a shows typical impedance data collected in coin

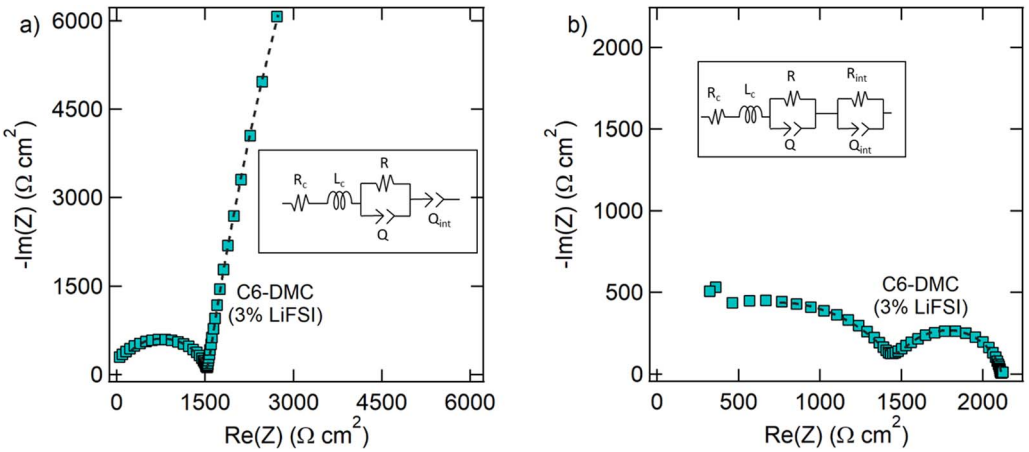

Figure 2. Typical impedance profiles and equivalent circuits for a) conductivity and b) Li symmetric samples. The dashed black lines are the fits to the equivalent circuits shown. Data collected at 30°C.

cells and the equivalent circuit is shown in the inset. R is the resistance of the electrolyte/separator composite, Q and Q_{int} are the constant phase elements associated with the electrolyte/separator and interface, respectively, and R_c and L_c are the resistance and inductance, respectively, associated with the VMP3 cables. The conductivity of the electrolyte was calculate using Equation 1

$$\sigma = c\frac{l}{RA} \quad [1]$$

where A is the electrode area of the coin cells in cm^2, l is the thickness of the separator in cm, and c is an empirically determined constant to account for the presence of the separator. The constant c was determined by measuring the conductivity of four electrolytes in a liquid cell described in Reference 22: C6-DMC with 3 wt% LiTFSI and C8-DMC with 3 wt% LiTFSI, C6-DMC with 20 wt% LiFSI, and C6-DMC with 15 wt% LiBETI at 30°C. The ratio of the measured conductivity in the liquid cell to that measured in the coin cell with the separator was 8.70 ± 0.06 for the four electrolytes.

Transference number cells were similar to the conductivity cells. However, instead of using stainless steel shims, lithium discs, cut from lithium chips (MTI Corp.), were used on either side of the electrolyte soaked Celgard. The diameter of the 150 μm thick Li disc was 12.7 mm. Three replicate cells were produced for each electrolyte. Data were collected on a Bio-Logic VMP3 potentiostat. Each sample cell was subjected to a conditioning treatment, which consisted of charge and discharge cycles at 0.02 mA/cm^2 in order to help stabilize the interfacial layer. The sequence performed was a 4 hour charge, 30 minutes rest, a 4 hour discharge, 30 minutes rest, and repeated for a total of 6 times. Ac impedance was carried out before the beginning of conditioning, after each rest step, and at the end of conditioning. Each sample was then polarized at $\Delta V = +/-40$ mV and $+/-80$ mV for 1 hour in order to ensure that the steady state transference number collected was independent of the applied potential. During chronopotentiometry, current was measured at 1 second intervals in order to capture the full current response. Ac impedance data were collected every 20 minutes with an ac amplitude of 20 mV and 40 mV for the dc applied potentials of $+/-40$ mV and $+/-80$ mV, respectively. The data obtained for all of these cases were similar. We report data acquired using ac impedance spectroscopy with an amplitude of 20 mV during dc polarization of 40. Data were modeled to the equivalent circuit shown in the inset of Figure 2b, where R_{int} was the interfacial resistance. Figure 2b represents the typical data seen for Li symmetric cells.

Assuming Ohm's law, which is a reasonable assumption prior to cell polarization due to a lack of concentration gradients, an initial current, I_Ω, is given by Equation 2:

$$I_\Omega = \frac{\Delta V}{R_T} \quad [2]$$

where ΔV is the applied polarization potential and R_T is the total initial cell resistance as measured by ac impedance spectroscopy. Equation 3 was then used to calculate the steady-state transference number:

$$t_{ss}^{+} = \frac{I_{ss}}{I_\Omega}\left(\frac{\Delta V - I_\Omega R_0}{\Delta V - I_{ss}R_{ss}}\right) \quad [3]$$

where I_{ss} is the steady state current, R_0 is the initial interfacial resistance, and R_{ss} is the interfacial resistance when I_{ss} is reached. The transference number alludes to how polarizable an electrolyte is, thus a transference number near unity suggests that concentration gradients do not build up within the electrolyte.

All electrochemical characterization experiments were conducted at 30°C.

Results and Discussion

The solubility limits for LiFSI, LiTFSI, and LiBETI in C6-DMC and C8-DMC are shown in Figure 3. The salts were added in 5 wt% increments until the solubility limit was reached. The solubility limit for each electrolyte was determined visually. Salts were assumed fully dissolved if the electrolyte was transparent, and phase separated if it was opaque. The solubility limit is taken as the average of the solution's salt concentration just below the solubility limit (transparent)

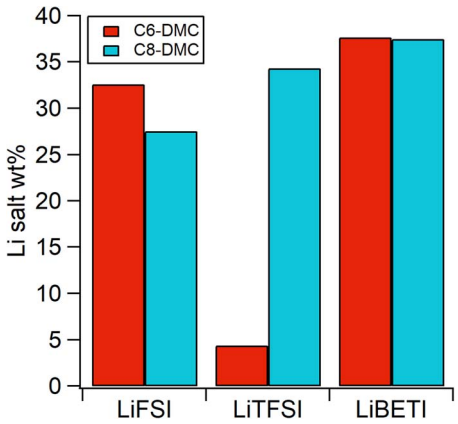

Figure 3. Li salt solubility in C6-DMC and C8-DMC as a function of salt wt%.

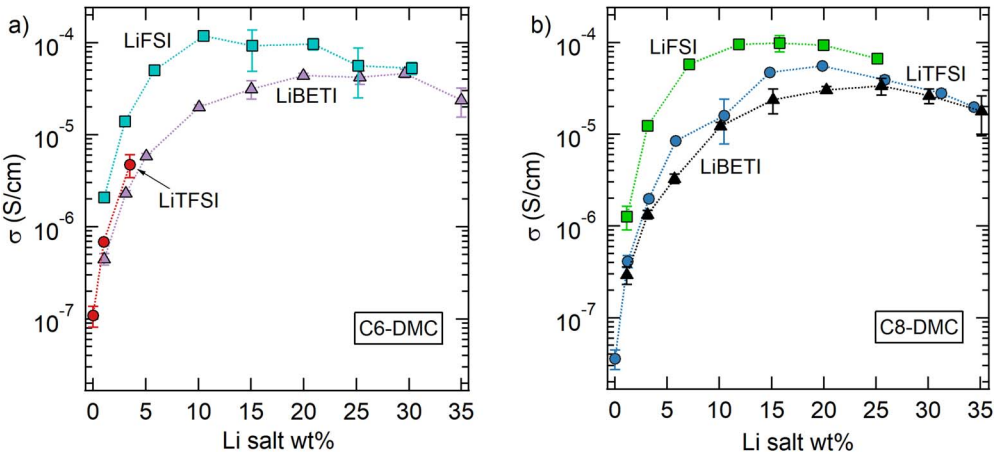

Figure 4. Conductivity of LiFSI, LiTFSI, and LiBETI in a) C6-DMC and b) C8-DMC. All data collected at 30°C.

and just above the solubility limit (opaque). Figure 3 shows the salt wt% for the six PFE/salt combinations. The solubility limit is a weak function of anion size for C8-DMC, increasing monotonically from 27.5 to 37.5 wt% in our experimental window. In uncharged systems, the entropy of mixing decreases with increasing molecular size, which, in turn, is expected to result in decreasing solubility limits. The observed trend in C8-DMC is not consistent with this expectation. It is possible that dissociation is favored in salts with large anions due to both lowering of lattice energy and charge delocalization, and that the observed trend in C8-DMC is due to this effect. The dependence of the solubility limit on anion size in C6-DMC is more interesting. The solubility of LiTFSI, the salt with an anion of intermediate size, is only 4.4 wt%, which is about an order of magnitude lower than that of all of the other five systems. This experiment was carried out three times in order to confirm the surprisingly low solubility limit in C6-DMC; all samples with LiTFSI concentrations from 5.3 to 29.9 wt% were phase-separated and opaque. Perhaps the entropic effects mentioned above are not entirely negligible in PFE electrolytes. The data in Figure 3 indicate that the interactions between the fluorinated lithium salts and perfluorinated electrolyte solvents are complex, and more work is required to establish the underpinnings of solubility.

The lithium salt that is predominant in the literature on PEO-based electrolytes, LiTFSI, cannot be used with C6-DMC. This suggests that replacing the hydrogen atom with fluorine has a large effect on electrolyte properties. All of our previous papers on perfluoropolyether (PFPE) electrolytes[7–11] are based on LiTFSI. However, the data in Figure 3 suggests that other salts might be better suited for perfluorinated electrolytes.

The dependence of conductivity, σ, on salt concentration for C6-DMC electrolytes, obtained with blocking electrodes, is shown in Figure 4a. The final datum for each data set represents the solubility limit. For LiFSI and LiBETI electrolytes, conductivity increases rapidly at low salt concentrations, goes through a shallow maximum, and decreases slightly at high salt concentrations. The limited solubility of TFSI- severely limits our measurement window in C6-DMC. Within the measurement window, however, the conductivity of LiTFSI- and LiBETI-based electrolytes are similar. At low salt concentrations, the conductivity of the LiFSI electrolyte is significantly higher than that of the others. The maximum conductivity of LiFSI in C6-DMC is 1×10^{-4} S/cm, which is also significantly higher than that of LiBETI in the same solvent. At high concentrations, however, the conductivities of the two systems are similar, see data at 30 wt% salt.

The dependence of conductivity, σ, on salt concentration for C8-DMC electrolytes, obtained with blocking electrodes, is shown in Figure 4b. All three electrolytes exhibit a shallow maximum with LiFSI exhibiting the highest conductivity followed by LiTFSI followed by LiBETI. At many salt concentrations, the conductivity of LiTFSI and LiBETI electrolytes in C8-DMC are within experimental error. This is especially true at salt concentrations $\geq$ 25 wt%. It appears as if the conductivity of the LiFSI electrolytes in C8-DMC would approach that of the other electrolytes at high salt

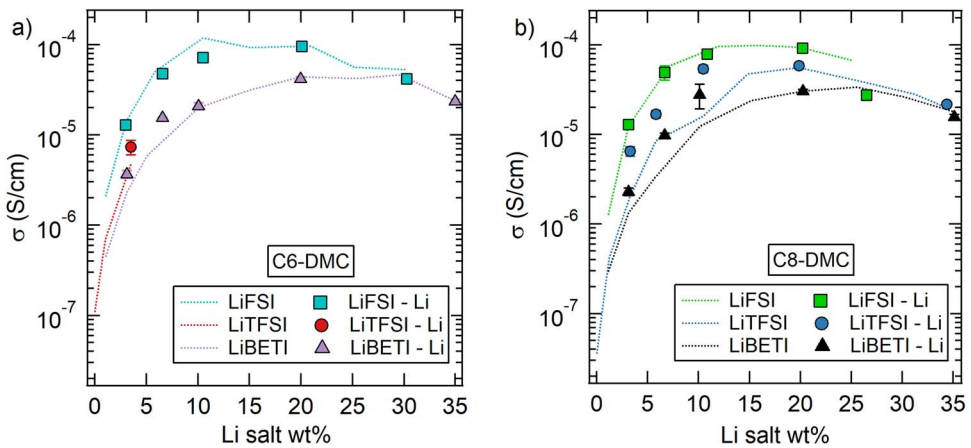

Figure 5. Conductivity values extracted from Li symmetric cells and compared to the results from the blocking electrodes for a) C6-DMC and b) C8-DMC. Markers and errors bars from the blocking electrodes were removed for clarity, but the blocking electrode conductivities can be seen as continuous lines. Conductivities calculated from non-blocking lithium electrodes are shown as symbols.

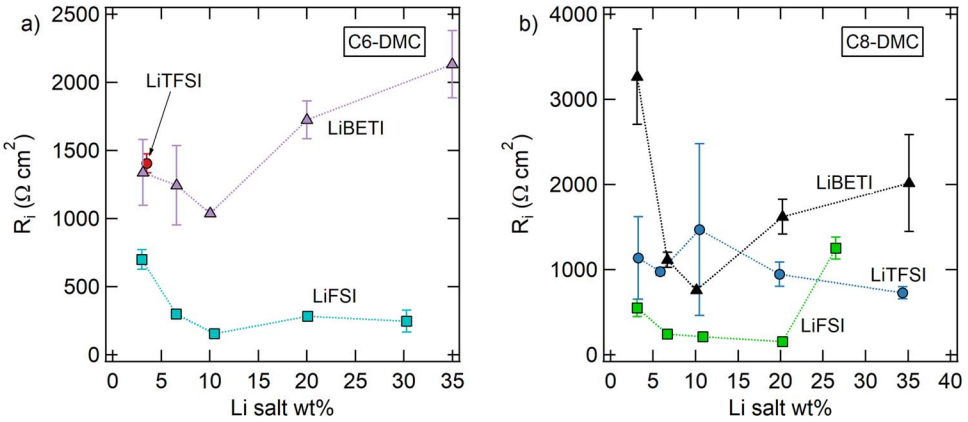

Figure 6. Final interfacial resistance as a function of Li salt concentration and type of Li salt for a) C6-DMC and b) C8-DMC.

concentrations (30–35 wt%), but a direct comparison is precluded by limited solubility (see Figure 4b).

For the case of amorphous PEO with methyl end groups (250 g/mol) and with 25 wt% LiTFSI, the maximum conductivity at 25°C is about 2×10^{-3} S/cm.[23] The maximum conductivity of PFE electrolytes is thus a factor of five lower than that of PEO electrolytes.

The symbols in Figures 5a and 5b show the dependence of conductivity, σ, on salt concentration for C6-DMC and C8-DMC electrolytes, obtained with non-blocking lithium metal electrodes. The continuous curves in Figure 5 show σ vs salt concentration obtained with blocking electrodes (Figure 4). In most cases, the conductivities determined with either blocking or non-blocking electrodes are similar. In principle, there should be no difference in conductivity values obtained using blocking or non-blocking electrodes. However, one might expect irreversible reactions between the fluorinated electrolytes and lithium metal to interfere with the conductivity measurements. It is evident that this is not the case. The irreversible reactions, however, do result in measurable interfacial resistances (Figure 2b).

The dependence of interfacial resistance, R_i, on salt concentration for C6-DMC is shown in Figure 6a. Due to the limited solubility of LiTFSI in C6-DMC, only one concentration was studied (3 wt% salt). At low salt concentrations, R_i for LiTFSI was similar to that of LiBETI in this solvent. Interestingly, the same can be said for conductivity (Figure 4a). For the soluble salts, LiFSI and LiBETI, R_i decreases with increasing salt concentration until R_i reaches a minimum at 10 wt%. At this concentration, for LiFSI, the minimum R_i for LiFSI is 155 ± 28 Ω cm^2. This is about an order of magnitude lower than that of LiBETI, which is 1040 ± 24.5 Ω cm^2. At concentrations between 10 wt% and the solubility limit, R_i of LiBETI increases dramatically to values as high as 2019 +/−569 Ω cm^2, while that of LiFSI approaches a plateau.

The dependence of interfacial resistance, R_i, on salt concentration for C8-DMC is shown in Figure 6b. R_i obtained from LiBETI exhibits a minimum that is similar to that obtained in C6-DMC (Figure 6a). R_i obtained from LiTFSI is independent of salt concentration (within experimental error). R_i obtained from LiFSI exhibits a shallow maximum with a minimum value of 154 ± 23 Ω cm^2 at 20 wt%. While the trends seen in Figure 6b are complex, at a given salt concentration, interfacial impedance generally decreases with decreasing anion size.

It is noteworthy that LiFSI/C6-DMC and LiFSI/C8-DMC, the systems that exhibit the highest conductivity, also exhibit the lowest interfacial impedance (Figures 4 and 6).

A significant motivation to the large number of published papers on lithium metal and PEO-based electrolytes is the stability of the solid-electrolyte interface that forms in these systems.[24,25] The interfacial impedance of lithium metal and PEO (MW = 4000 kg/mol) with LiBETI was measured by Appetecchi, G. B. et al.[26] They report a minimum of 80 Ω cm^2 in an electrolyte with 20 wt% salt. In another study by Zhang, H. et al. on LiFSI and LiTFSI in PEO (MW = 5000 kg/mol) at concentrations of 17.5 and 24.5 wt%, R_i values of 80 Ω cm^2 and 325 Ω cm^2 were obtained, respectively.[27] The values of R_i reported in our study for LiFSI/PFE systems are thus similar to those of LiFSI/PEO, and significantly lower than that of LiTFSI/PEO. The interfacial resistances that were measured in the PEO electrolytes in References 26 and 27 were obtained without the passage of current. In contrast, the values reported in Figure 6 were obtained after the passage of current; see details about conditioning cycles in Electrolyte preparation section (Experimental characterization). The differences in R_i of PFE and PEO electrolytes could also be due to differences in hydrophilicity and the presence of trace amounts water.[28]

Figures 7a and 7b show the current obtained upon application of a dc potential of 40 mV in C6-DMC and C8-DMC electrolytes. The data shown here were obtained from solutions of LiFSI, LiTFSI, and LiBETI at a salt concentration of 3 wt% for both electrolytes. In all cases, the current obtained at early times is slightly higher than that obtained at steady-state. The steady-state current, I_{ss}, obtained at $t >$ 10 min, is highest for LiFSI, followed by LiTFSI and then LiBETI. I_{ss} is governed by electrolyte conductivity, interfacial impedance, and other transport properties, namely the salt diffusion coefficient and transference number.[29] The data in Figure 7 enable calculation of the approximate transference number based on steady-state current, t^+_{ss}, using Equations 2 and 3.

Figure 8a plots t^+_{ss} against salt concentration for C6-DMC. At the lowest salt concentration (3 wt%), all three electrolytes exhibit t^+_{ss} values near unity (between 0.93 and 0.98). For the soluble salts, LiFSI and LiBETI, t^+_{ss} decreases with increasing salt concentration. The LiFSI electrolytes reach a minimum of 0.64 ± 0.03 at 30 wt%, while the LiBETI electrolytes reach a minimum of 0.82 ± 0.02 at 35 wt%. Figure 8b plots t^+_{ss} against salt concentration for C8-DMC. For LiBETI and LiTFSI, t^+_{ss} decreases with increasing salt concentration. For LiFSI, t^+_{ss} reaches a minimum of 0.73 ± 0.05 at 20 wt%. Over most of the experimental window, t^+_{ss}, at a given salt concentration, increases with anion size: BETI- > TFSI- > FSI-. This result is expected as larger ions should be less mobile.

Of note is that even though LiFSI has the lowest t^+_{ss} value in this study, it is still greater than 0.6 in C6-DMC and greater than 0.7 in C8-DMC across all concentrations. This is still much higher than PEO-based electrolytes wherein t^+_{ss} values are reported to be in the range of 0.1–0.4.[30] Furthermore, t^+_{ss} values for C8-DMC electrolytes are higher than those for C6-DMC electrolytes. In previous work, it was shown that t^+_{ss} for a 9.1 wt% LiTFSI in PFPE with DMC endgroups (MW = 1.1 kg/mol) was 0.9,[8] which is higher than that of 10 wt% LiTFSI in C8-DMC. These observations suggest that t^+_{ss} increases with increasing molecular weight. In contrast, t^+_{ss} of PEO-based electrolytes decrease with increasing molecular weight.[30] The presence of specific interactions between PEO and Li cations is well-established, and this effect is used to describe the dependence of t^+_{ss}

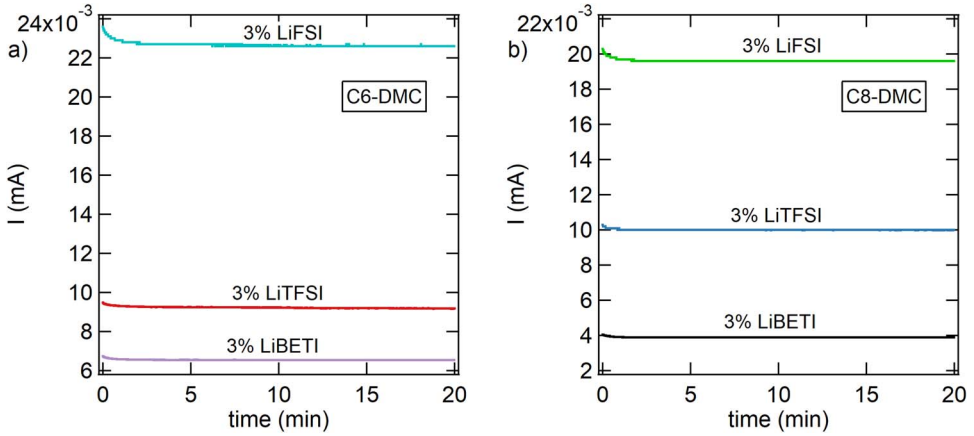

Figure 7. Typical current vs time profile for a) C6-DMC and b) C8-DMC as a function of Li salt. Notice that the steady-state current is a strong function of the anion.

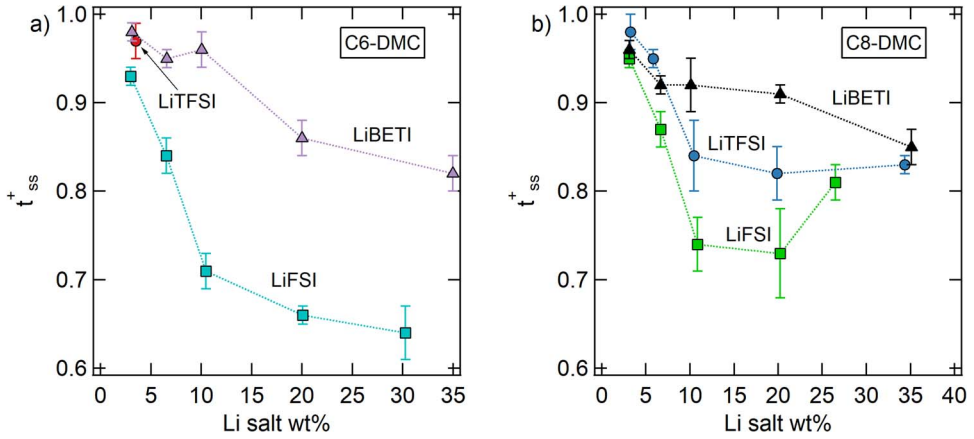

Figure 8. Steady-state transference number for a) C6-DMC and b) C8-DMC as a function of Li salt and Li salt wt%.

and molecular weight.[31] Our observations in PFPE electrolytes thus suggest the presence of specific interactions between the anions and the fluorinated backbone.

Figures 4 and 8 indicate that increasing salt concentration has opposite effects on σ and t^+_{ss}: σ generally increases while t^+_{ss} generally decreases with salt concentration. In practical applications, the current through an electrolyte under an applied dc potential is the important metric. This metric is proportional to the product σt^+_{ss}.[14,16,31,32] Figures 9a and 9b show the dependence of σt^+_{ss} on salt concentration. A maximum is observed in the vicinity of 20 wt% salt in both C6-DMC and C8-DMC, irrespective of the soluble salt used. The optimal value of σt^+_{ss} in PFE electrolytes, 7×10^{-5} S/cm, is lower than that of PEO-based electrolytes, which are in the range of 2×10^{-4} to 5×10^{-4} S/cm. Additionally, σt^+_{ss} of LiFSI in C8-DMC is within experimental error of LiFSI in C6-DMC, even though C8-DMC is of a higher molecular weight. It is evident that the optimal salt concentration for our PFE electrolytes is 20 wt%; neither σ nor t^+_{ss} is maximized at this concentration.

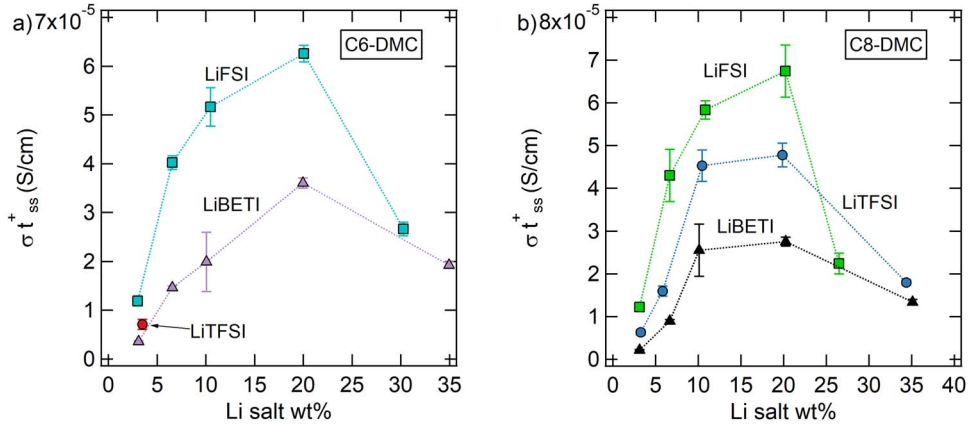

Figure 9. Conductivity of the Li cation for a) C6-DMC and b) C8-DMC as a function of Li salt and Li salt wt%.

Conclusions

The effect of anion size on ion transport in perfluoropolyether electrolytes was studied by examining mixtures of LiFSI, LiTFSI, and LiBETI in C6-DMC and C8-DMC. The solubility limit of all systems was in the 25–35 wt% range except for LiTFSI in C6-DMC, which was 4.4 wt%. Electrolytes with LiFSI exhibited the highest conductivity, σ, and lowest interfacial impedance. However, their steady-state transference number, t^+_{ss}, was lower than that of the other two salts. The efficacy of the electrolytes was studied by examining the product, σt^+_{ss}. The optimal salt concentration was 20 wt% in all cases (except the system with limited salt solubility). Of the salts studied, LiFSI-based systems exhibited the highest value of σt^+_{ss}. Our work suggests that specific interactions between the anions and the fluorinated backbones of our solvents may be important. Further spectroscopic and computational studies to examine these effects seem warranted.

Acknowledgments

This project is primarily funded by the National Science Foundation, grant Number 1505669, under the SusChEM initiative, which supported the work of D.B.S., A.K., and N.P.B. The work of K.R.O., S.J.M., and J.D.S. was supported as part of the Center for Mesoscale Transport Properties, an Energy Frontier Research Center supported by the U.S. Department of Energy, Office of Science, Basic Energy Sciences, under award #DE-SC0012673.

List of Symbols

A	Active surface area of electrode; (cm^2)
c	Ratio between liquid cells and coin cells; (unitless)
I_{ss}	Steady-state current; (mA)
I_o	Initial current; (mA)
l	Thickness of separator; (cm)
L_c	Inductance of measurement cabling
Q_{el}	Constant phase element of the electrolyte
Q_{int}	Constant phase element of the interface
R_c	Resistance of measurement cabling; (Ω)
R_{el}	Resistance of electrolyte; (Ω)
R_{int}	Resistance of solvent/electrode interface; (Ω)
R_o	Resistance of solvent/electrode interface initially, prior to polarization; (Ω)
R_{ss}	Resistance of solvent/electrode interface when I_{ss} reached; (Ω)
t^+_{ss}	Steady-state transference number

Greek

σ	Conductivity of the electrolyte; (S/cm)
δt^+	Standard deviation in t^+
δσ	Standard deviation in σ; (S/cm)

ORCID

Deep B. Shah https://orcid.org/0000-0001-7816-031X

References

1. J. B. Goodenough and Y. Kim, *Chem. Mater.*, **22**, 587 (2010).
2. D. Aurbach, E. Zinigrad, Y. Cohen, and H. Teller, *Solid State Ionics*, **148**, 405 (2002).
3. V. Eshkenazi, E. Peled, L. Burstein, and D. Golodnitsky, *Solid State Ionics*, **170**, 83 (2004).
4. A. Kraytsberg and Y. Ein-Eli, *Adv. Energy Mater.*, **2**, 922, (2012).
5. L. Yang, B. Ravdel, and B. L. Lucht, *Electrochem. Solid-State Lett.*, **13**, A95 (2010).
6. Z. Zhang, L. Hu, H. Wu, W. Weng, M. Koh, P. C. Redfern, L. A. Curtiss, and K. Amine, *Energy Environ. Sci.*, **6**, 1806 (2013).
7. D. H. C. Wong, J. L. Thelen, Y. Fu, D. Devaux, A. A. Pandya, V. S. Battaglia, N. P. Balsara, and J. M DeSimone, *Proc. Natl. Acad. Sci.*, **111**, 3327 (2014).
8. M. Chintapalli, K. Timachova, K. R. Olson, S. J. Mecham, D. Devaux, J. M. DeSimone, and N. P. Balsara, *Macromolecules*, **49**, 3508 (2016).
9. D. H. C. Wong, A. Vitale, D. Devaux, A. Taylor, A. A. Pandya, D. T. Hallinan, J. L. Thelen, S. J. Mecham, S. F. Lux, A. M. Lapides, P. R. Resnick, T. J. Meyer, R. M. Kostecki, N. P. Balsara, and J. M. Desimone, *Chem. Mater.*, **27**, 597 (2015).
10. K. Timachova, M. Chintapalli, K. R. Olson, S. J. Mecham, J. M. DeSimone, and N. P. Balsara, *Soft Matter*, **13**, 5389 (2017).
11. K. R. Olson, D. H. C. Wong, M. Chintapalli, K. Timachova, R. Janusziewicz, W. F. M. Daniel, S. Mecham, S. Sheiko, N. P. Balsara, and J. M. DeSimone, *Polymer*, **100**, 126 (2016).
12. R. Berger, G. Resnati, P. Metangolo, E. Weber, and J. Hulliger, *Chem. Soc. Rev.*, **40**, 3496 (2011).
13. E. Cznotka, S. Jeschke, M. Grünebaum, and H. D. Wiemhöfer, *Solid State Ionics*, **292**, 45 (2016).
14. M. Watanabe, S. Nagano, K. Sanui, and N. Ogata, *Solid State Ionics*, **2830**, 911 (1988).
15. P. G. Bruce and C. A. Vincent, *J. Electroanal. Chem.*, **225**, 1 (1987).
16. J. Evans, C. A. Vincent, and P. G. Bruce, *Polymer*, **28**, 2324 (1987).
17. S. Lascaud, M. Perrier, A. Vallee, S. Besner, J. Prudhomme, and M. Armand, *Macromolecules*, **27**, 7469 (1994).
18. W. Gorecki, M. Jeannin, E. Belorizky, C. Roux, and M. Armand, *J. Phys. Condens. Matter*, **7**, 6823 (1995).
19. A. Vallee, S. Besner, and J. Prud'Homme, *Electrochim. Acta*, **37**, 1579 (1992).
20. K. Pozyczka, M. Marzantowicz, J. R. Dygas, and F. Krok, *Electrochim. Acta*, **227**, 127 (2017).
21. D. O'Hagan, *Chem. Soc. Rev.*, **37**, 308 (2008).
22. A. A. Teran, M. H. Tang, S. A. Mullin, and N. P. Balsara, *Solid State Ionics*, **203**, 18 (2011).
23. J. Zhou and P. S. Fedkiw, *Solid State Ionics*, **166**, 275 (2004).
24. E. Paled, *J. Electrochem. Soc.*, **126**, 2047 (1979).
25. P. Verma, P. Maire, and P. Novák, *Electrochim. Acta*, **55**, 6332 (2010).
26. G. B. Appetecchi and S. Passerini, *J. Electrochem. Soc.*, **149**, A891 (2002).
27. H. Zhang, C. Liu, L. Zheng, F. Xu, W. Feng, H. Li, X. Huang, M. Armand, J. Nie, and Z. Zhou, *Electrochim. Acta*, **133**, 529 (2014).
28. C. Xu, B. Sun, T. Gustafsson, K. Edström, D. Brandell, and M. Hahlin, *J. Mater. Chem. A*, **2**, 7256 (2014).
29. M. Doyle and J. Newman, *J. Electrochem. Soc.*, **142**, 3465 (1995).
30. D. Devaux, R. Bouchet, D. Glé, and R. Denoyel, *Solid State Ionics*, **227**, 119 (2012).
31. A. Maitra and A. Heuer, *Phys. Rev. Lett.*, **98**, 227802 (2007).
32. N. P. Balsara and J. Newman, *J. Electrochem. Soc.*, **162**, A2720 (2015).